Journal of Thermal Analysis and Calorimetry
https://doi.org/10.1007/s10973-026-15588-z

Numerical analysis and transient thermal modeling of microwave dehydration of tomato: validation with experimental results

Emre Arpaci[1] · Ş. Özgür Atayılmaz[1] · Zafer Gemici[1] · Hakan Demir[1]

Received: 7 August 2025 / Accepted: 24 April 2026
© The Author(s) 2026

Abstract

In this study, a model of microwave dehydration of tomato slices was created. The model illustrates the temperature variations during the microwave dehydration of tomatoes by accounting for the moisture transport effect, while also demonstrating the electric field distribution and volume loss density. Model validation was carried out by experimental tests, and the absolute mean error was found to be 3.55 and 5.73 °C for 210 and 350W power levels, respectively. To reach more precise solutions, the thermophysical and dielectric properties of tomatoes were assumed to be temperature dependent. To explore drying kinetics and moisture transport in microwave drying, experimental results of tomato slices (5 mm thick) dried at 210 and 350W power are compared with four models, including three thin-layer drying models (Henderson–Pabis, Page, and Wang & Singh) and Fick's diffusion model. The Page and Wang Sing model was found to be in outstanding consensus with the empirical data in microwave drying process. The reasons for the poorer fit of the Fick model compared to the other models were explained. In addition, the difficulties of microwave dehydration CFD modeling and future recommendations were explained in detail. The findings and frameworks presented herein offer substantial knowledge that may broaden the investigative horizons of researchers within this subject.

Keywords Microwave dehydration CFD modeling · Drying kinetics

List of symbols

E	The electric field intensity
ε	Permittivity
ε'	The real permittivity
ε''	The dielectric loss factor
ε_0	Permittivity of free space or well-known as vacuum permittivity
RMSE	Root mean square error
ω	Angular frequency
σ	Conductivity
$\tan\delta$	Dielectric loss tangent
MAE	Mean absolute error
MR	Moisture ratio
MR_{exp}	Empirical moisture ratio
MR_{pred}	Model-predicted moisture ratio
P	Average absorbed power

✉ Emre Arpaci
earpaci@yildiz.edu.tr

[1] Department of Mechanical Engineering, Faculty of Mechanical Engineering, Yildiz Technical University, Yildiz, 34349 Istanbul, Turkey

Introduction

Microwave drying is a process that utilizes microwave energy to remove moisture from the products and is widely used in the food industry [1, 2], pharmaceuticals [3], fossil fuel handling [4], and other fields [5, 6]. There is no doubt that microwave drying has attracted the attention of researchers from almost every engineering discipline. Microwaves (MW) directly heat the interior of products, enabling faster, more uniform drying compared to traditional drying methods that rely on surface heat transfer. Microwave drying principle relies on volumetric and dielectric heating. The microwave is a fast-heating mode that utilizes electromagnetic radiation with a wavelength of 1m to 1 mm and a frequency range of 300 MHz–300 GHz. The magnetron generates electromagnetic waves or microwaves. Microwaves generate heat as a consequence of the interaction between the food products and the microwaves [7]. Microwaves cause polar molecules such as water to vibrate rapidly, generating internal heat and evaporating moisture. Because microwaves penetrate deeply into the material, drying is generally more uniform than in surface-heating methods like convective drying. However, despite its advantages, microwave drying

Published online: 14 May 2026

can still produce uneven heating, especially in heterogeneous materials, leading to localized overheating or hot spots [8]. A hot spot can be defined as a tiny area of the geometry that is significantly hotter than the rest of the region. Differences in microwave absorption properties of heated products may create hot spots, causing uneven temperature distribution during microwave heating. Hot-spot effects are valuable in microwave operations, although it is challenging to measure accurately and there have not been many quantitative reports [9]. Combining microwave drying with additional drying processes such as convection drying, vacuum drying, fluidized bed drying, and freeze-drying may lessen the problems in microwave drying [10, 11]. Different products interact with microwaves in different behavior, such as reflecting, transmitting, or absorbing. Dielectric dissipation is a main factor in determining a material's microwave absorption capability. Composite materials can experience selective heating during microwave exposure, leading to non-uniform temperature distribution due to variations in absorption [9]. MW technique is extensively utilized in drying applications of various agricultural goods like apple [12], banana [13], tomato [14].

The tomato is one of the most broadly cultivated vegetables in the world. It is incredibly adaptable and can be utilized in an extensive range of industrial and culinary procedures [15], some of these common uses: fresh consumption, juices and drinks, salsas and dips, tomato puree, tomato paste, ketchup; also, tomatoes are a good source of dietary fiber and vitamin C, vitamin K, potassium, and folate may all be found in tomatoes. Therefore, the numerical model presented in this study for the microwave drying process of tomatoes, one of the most broadly utilized vegetables, will help understand the entire process and provide a new perspective to researchers working in the field of MW drying.

A valuable method for lessening the thermal impact on tomato products is microwave drying [16]. A study exposed that certain of the qualitative features of dried tomatoes were preserved when predried utilizing microwaves with different power densities. For the agro-food processing, applying microwave power densities before the oven-drying process may therefore be an alternative strategy for commercializing high-quality dried tomatoes [17]. Also, in terms of drying time and energy usage, microwave drying alone outperformed the convective approach in a study [18]. A study investigates the impact of drying parameters (microwave power, drying air temperature, and thickness) on some physicochemical properties of dried tomato pulp powder, as well as optimizing the drying parameters for individual quality attributes and overall quality, utilizing response surface methodology based on various responses (drying time, pH, acidity, vitamin C content, and color difference). The kinetics and mass transfer modeling of the drying tests were also investigated. Based on the empirical results, microwave drying of foamed tomato pulp considerably lowered drying time. The impact of foam thickness and air temperature was also notable [19]. A research assessed the impact of processing combinations, slice thickness, pretreatments, and microwave power on the quality metrics of microwave-dried tomatoes. In that study, these pretreatments procedures utilized: Twelve (12) kg of tomatoes were treated to each water blanching (WB) for 1 min, 5% wv^{-1} ascorbic acid treatment (AA), and 5% wv^{-1} sodium metabisulphite treatment (SM) for 5 min. The tomato pretreated with WB exhibited the highest shrinking, followed by those treated with AA and SM. Shrinkage increased as tomato slice thickness rose. SM pretreatment of tomatoes at 6 mm thickness and 90W processing power led to the highest rehydration ratio and β-carotene retention. On the contrary, the combination of SM pretreatment, 4 mm thickness, and 360W processing power caused to the maximum retention of lycopene and ascorbic acid within the experimental range. The forecasted models were empirically evaluated and found to be in good consistency with empirical values [20]. These studies demonstrate that microwave drying of tomatoes is a preferred method and has various advantages. In this study, a numerical model of microwave drying tomatoes was presented, and the intention was to offer researchers an understanding of the microwave drying process by presenting the numerical model of microwave drying and its compatibility with experimental data.

Microwave drying can be numerically modeled by simulating the complicated interactions that exist between electromagnetic fields, mass transport, and heat transfer throughout the drying procedures. Researchers have conducted several numerical studies on microwave drying and tried to present new developments. These are basically efforts to understand microwave process and model the realistic microwave drying simulation and investigate the compatibility of parameters like temperature and humidity change with experimental data. Several approaches and methodologies have been utilized for numerical models in microwave drying, such as finite element method (FEM), Multiphysics software (e.g., ANSYS HFSS and COMSOL Multiphysics), specialized models, and finite difference method (FDM). These methodologies for numerical models in microwave drying are explained below briefly.

Finite Element Method (FEM): The electromagnetic field in microwave drying systems is modeled utilizing this technique, especially for dielectric materials that include losses. A FEM model is presented for the microwave combination washer dryer by Smit et al. [21]. It is reported that initial findings suggest that the system is accurately represented by the FEM model.

Finite Difference Method (FDM): The partial differential equations of mass, momentum, and heat are commonly solved utilizing the finite difference and finite element

approaches in numerical modeling of microwave drying. Finite difference approaches are commonly the method of choice when the problem involves a simple (regular) geometry because they are simple to formulate, even if the finite element method offers greater flexibility for modeling irregular geometries [22].

Program for Multiphysics: Multiphase flow in porous material during microwave drying is simulated utilizing multiphysics. Multiphysics software (like COMSOL Multiphysics, ANSYS HFSS) is often used to visualize the solutions and obtain results swiftly [23, 24].

Specialized models: Special numerical models can be required for materials such as ceramics, wood, and different agricultural products in numerical models of microwave drying. Moreover, researchers build their own numerical microwave drying models that are compatible with experimental tests [25, 26].

In Table 1, some numerical studies and main findings that may be notable in understanding the crucial points for the topic are shown. The results obtained from these studies briefly show that different simulation programs and artificial neural networks were utilized for numerical analysis in the microwave drying process.

In this study, VOSviewer (version 1.6.20) was utilized to visualize author and index keywords and identify research trends in numerical modeling of microwave drying. A Web of Science search for "numerical models in microwave drying" yielded 277 publications covering the years 1983–2025. From their abstracts, VOSviewer identified 117 frequently used terms, grouped into fourteen distinct clusters, highlighting major research focuses and gaps in existing numerical models. In these abstracts, the most repeatedly utilized terms are "numerical modeling," "combined heating and drying," "combined dehydration," "combined microwave convective drying," "freeze-drying," and "boxthorn fruits." It shows that studies about microwave drying combined with other drying methods were more common. Each word's frequency of occurrence is displayed by the size of the circle beneath it. To help with their classification, distinct groups of closely related terms were illustrated utilizing a variety of colors. Data were retrieved from the Web of Science (WOS) database to visualize the term "cloud" using VOSviewer software, as shown in Fig. 1.

Comprehensive literature research showed that numerical models are widely utilized in microwave drying processes. In this study, a numerical model close to real experimental tests was created. The extensively utilized Ansys Electronics Desktop software and Ansys transient thermal were used. Thanks to this model, the microwave drying process will be better understood and the consequences of input parameters such as microwave power on the drying product will be simulated quickly. In this study, it was considered that the thermophysical properties of the dried product (tomato) changed depending on the temperature, and these properties were transferred to the model, with the intention of providing a better fit with the experimental results. Four popular drying models—three thin-layer models (Henderson–Pabis, Page, and Wang & Singh) and Fick's diffusion model—are compared with experimental data for tomato slices (5 mm thick) and dried at 210 and 350W microwave power to investigate drying kinetics in microwave drying. The compatibility of these four models with experimental data was investigated, and the pros and cons of the models were discussed.

Experimental procedure

A domestic microwave oven with adjustable microwave power level and timer was utilized for experimental studies, as shown in Fig. 2a. The microwave, operating at 2.45 GHz, was adjusted to 210 and 350W for experimental trials. Tomatoes were cut into 5-mm-thick slices utilizing a mandolin for all experiments. To determine the drying kinetics, the mass of tomato slices is measured with an electronic analytical and precision balance which has 10 mg resolution, as depicted in Fig. 2b. The temperature of the center slices is measured with an infrared thermometer every 30s. The microwave oven door was opened, the temperature of the middle slice was immediately measured with an infrared thermometer, and the door was closed. Infrared thermometer with laser marking has a resolution of 0.1 °C and an accuracy of ± 1.5 °C**,** as shown in Fig. 2c. The average temperature of the center slice tomato values found in the CFD was compared by measuring the temperature of the same slice with an infrared thermometer.

Numerical model

The suggested model was created to evaluate microwave heating processes for tomato in a domestic microwave utilizing Ansys Electronics Desktop and Workbench. A HP workstation with 64-GB RAM, Intel(R) Xeon(R) CPU E5-2630 v4, 2.20 GHz, and 2.20 GHz double processors was employed for this study. The HFSS model was generated in Ansys Electronics Desktop 2025, then transferred to the Ansys Workbench, and coupled to the transient thermal module. In that section, we will go over the numerical model comprehensively. Additionally, the mean absolute error (MAE) was employed as a parameter to assess the CFD model's prediction ability with respect to temperature distribution. An intuitive indicator of the model's precision in forecasting thermal behavior during the drying process, MAE, estimates the average absolute difference between the temperature values measured experimental results and those simulated. MAE mathematical expression is given:

Table 1 An overview table of numerical models for microwave drying

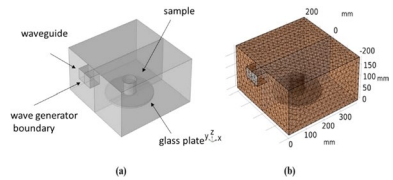
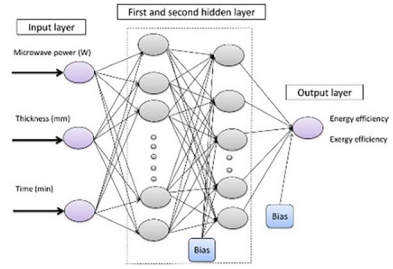
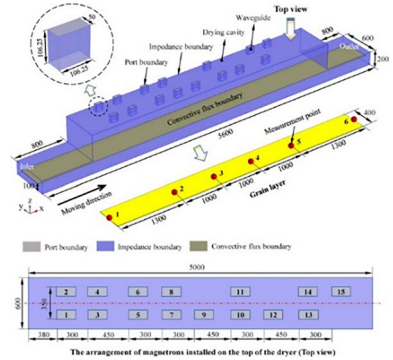
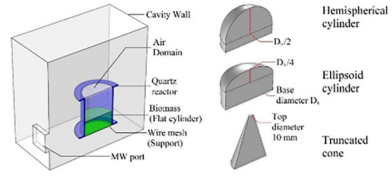
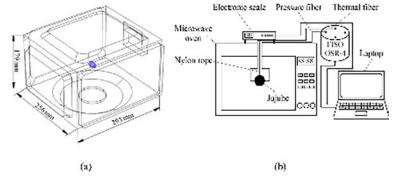
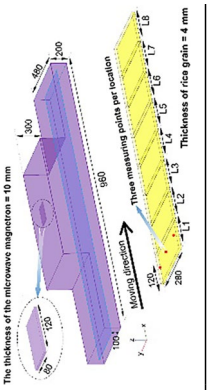
Authors	Brief overview	Main findings	Geometry
Tauhiduzzaman et al. [27]	A developed model to predict moisture loss under varying shapes and power regardless of shape and microwave power	Accurate waveguide sizing led to precise predictions of water heating times for various volumes, showing energy distribution patterns for high and low temperatures around an average of 100 °C	
Beigi et al. [28]	A domestic microwave oven was utilized to dry the onion slices, and the impact of sample thickness and power level on energy and exergy metrics was analyzed	Thick samples and higher microwave power levels greatly enhance efficiency, which substantially lessen the environmental effect of the drying process	
Shen et al. [29]	Utilizing numerical computation and experiments, heat and mass transport were investigated to acquire a better understanding of the drying behavior and continuous microwave drying of germinated brown rice (GBR)	Efficiently managing microwave energy during different drying stages can enhance drying efficiency and optimize energy utilization	
Siddique and Salema [30]	COMSOL Multiphysics was utilized for simulating the biomass materials heating under microwave drying, varying cylinder diameters (30–140 mm) with constant biomass volume across four shapes: cone, hemisphere, ellipsoid, and flat cylinder	The size and form of a cylindrical reactor with low-temperature dispersion and high MW power absorption for both low- and high-loss materials are highlighted in that study. It is significant because it illustrates how biomass turns into biochar, changing the dielectric characteristics from low loss to high loss as it heats up, which affects efficiency	
Hou et al. [31]	To simulate the intermittent microwave drying of a single jujube with two different moisture levels, a three-dimensional numerical model was created	As the MW power level and duty cycles increased through intermittent MW drying, the temperature and moisture losses of the samples also increased. As well, lower duty cycles produced better uniformity in both temperature and moisture content	

Table 1 (continued)

Authors	Brief overview	Main findings	Geometry
Li et al. [32]	This study presents a simulation strategy to sensibly examine temperature and moisture variations in a continuous microwave rice grain drying system. Also, the study develops a three-dimensional model that encompasses multiple physical fields, including heat and mass transfer electromagnetism	As microwave intensity increases, both the drying rate and temperature of the rice also rise. According to the findings, the drying rate has a positive correlation with temperature and an inverse relationship with material thickness	

$$\mathrm{MAE} = \frac{1}{N}\sum_{i=1}^{N}|T_{\mathrm{exp,i}} - T_{\mathrm{cfdsim,i}}| \quad (1)$$

In that equation, T_{exp} refers to the temperatures from the experiment, and T_{cfdsim} refers to the temperatures from the CFD results, and N is the number of the dataset of experiment result and CFD.

Model assumptions and geometry

A 3D outline of a microwave was created for the computational model as displayed in Fig. 3. The dimensions of the microwave oven sketch were 270 mm × 292 mm × 176 mm. A rectangular wave guide operating at a frequency of 2.45 GHz was placed on the top of the microwave. Dried tomatoes were drawn in 5 mm thickness. The tray was modeled as glass in the microwave oven. The microwave runs at 210 and 350W and is input via the rectangular port on the waveguide. The initial temperatures of the tomato slices were 22 and 24 °C for 210 and 350W, respectively, as in the experimental conditions.

Tomato slices' dielectric and thermophysical characteristics are thought to be temperature dependent. The CFD simulation is run for the period of 1–150s. Therefore, the thermophysical properties are considered to depend only on the temperature and not on the moisture content. Tomato's thermophysical and electromagnetic properties are compiled from literature surveys [33–36] and displayed in Table 2.

To simplify the model and boost the pace of convergence, the following assumptions were set up:

- Assuming that the medium is completely transparent for microwave propagation and that the air domain absorbs extremely little microwave energy.
- Air movement inside the microwave oven is assumed to be by natural convection, and it is a compressible fluid.
- The system initially was 22 and 24 °C for 210 and 350 W power, respectively.
- Heat losses due to moisture evaporation were acquired from the empirical results and added to the CFD simulations. In the empirical tests, the mass change was recorded. The heat effect of the amount of moisture lost was added to the CFD as a negative load for 210 and 350 W.

Meshing

Here physical preference is set to CFD; solver preference is fluent. The element size is 5 mm. There are 379,491 mesh and 85,567 nodes in the microwave model as depicted in Fig. 4a. The mesh element quality assessment is depicted in Fig. 5. The degree to which a mesh element's shape resembles the "ideal" shape is known as element quality, and skewness uses

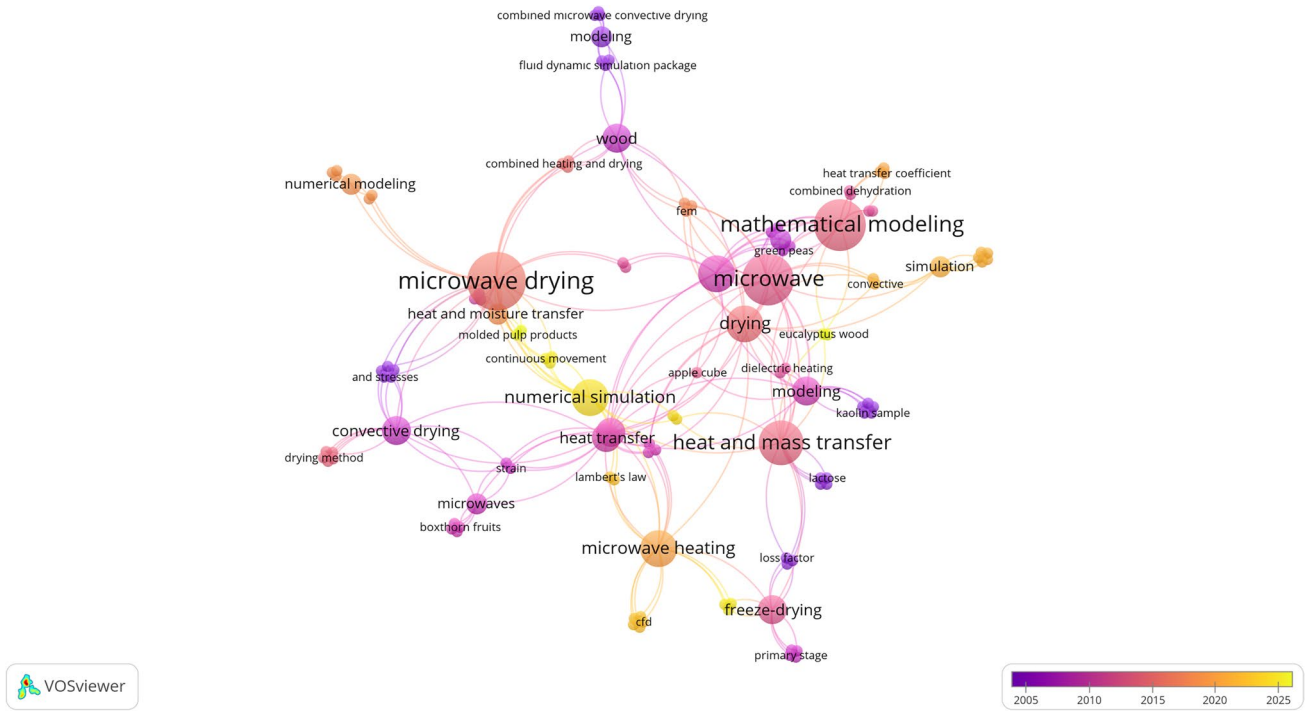


Fig. 1 Analysis of term co-occurrences based on abstracts for the research "Numerical models in microwave drying"

angle or geometric distortion to calculate how far a mesh element deviates from its ideal shape. Important criteria including mesh skewness and element quality were utilized to evaluate the computational mesh's quality. The average element quality in this study is 0.83863, as depicted in Fig. 5, which suggests a highly regular and well-shaped mesh. Furthermore, the mesh elements appear to have little angular distortion, as indicated by the average skewness value of 0.22539, which is within the excellent range. The mesh's high quality and suitability for computational fluid dynamics (CFD) simulations are confirmed by these numbers.

Basics of operations

When microwave energy strikes dielectric materials, it causes molecules or ion-pair dipoles to rotate, which is then converted to heat. The following terms convey the polarizing principles of these processes:

$$\varepsilon = \varepsilon_0 \varepsilon_r = \varepsilon_0(\varepsilon' - j\varepsilon'') \tag{2}$$

$$\varepsilon' = \frac{\sigma}{\omega \varepsilon_0} \tag{3}$$

$$\tan\delta = \frac{\varepsilon''}{\varepsilon'} \tag{4}$$

In these equations where;

ε: permittivity.

ε': the real permittivity.

ε'': the dielectric loss factor.

ε_0: permittivity of free space or well-known as vacuum permittivity.

ω: angular frequency.

σ: conductivity.

tanδ: dielectric loss tangent.

In the case of that the dielectric loss tangents tan (δ) of materials, which show the capability of the materials to be polarized at a given frequency, and temperature is smaller than 0.01, material is dielectric.

Accordingly, the average absorbed power (P) of the materials can be computed utilizing Eq. 5 [37], once the electric field intensity (E) and the microwave's angular frequency (ω) are known.

$$P = \omega \varepsilon_0 \varepsilon'' E^2 = \omega \varepsilon_0 \varepsilon' \tan\delta E^2 \tag{5}$$

Drying kinetics

To explain the drying behavior of 5-mm-thick tomato slices under microwave drying at 210 and 350W, four commonly utilized drying models were employed and compared with experimental data. These models were the Page model, Fick's diffusion model, Wang & Singh model, and Henderson & Pabis model. These models express the variation of the moisture

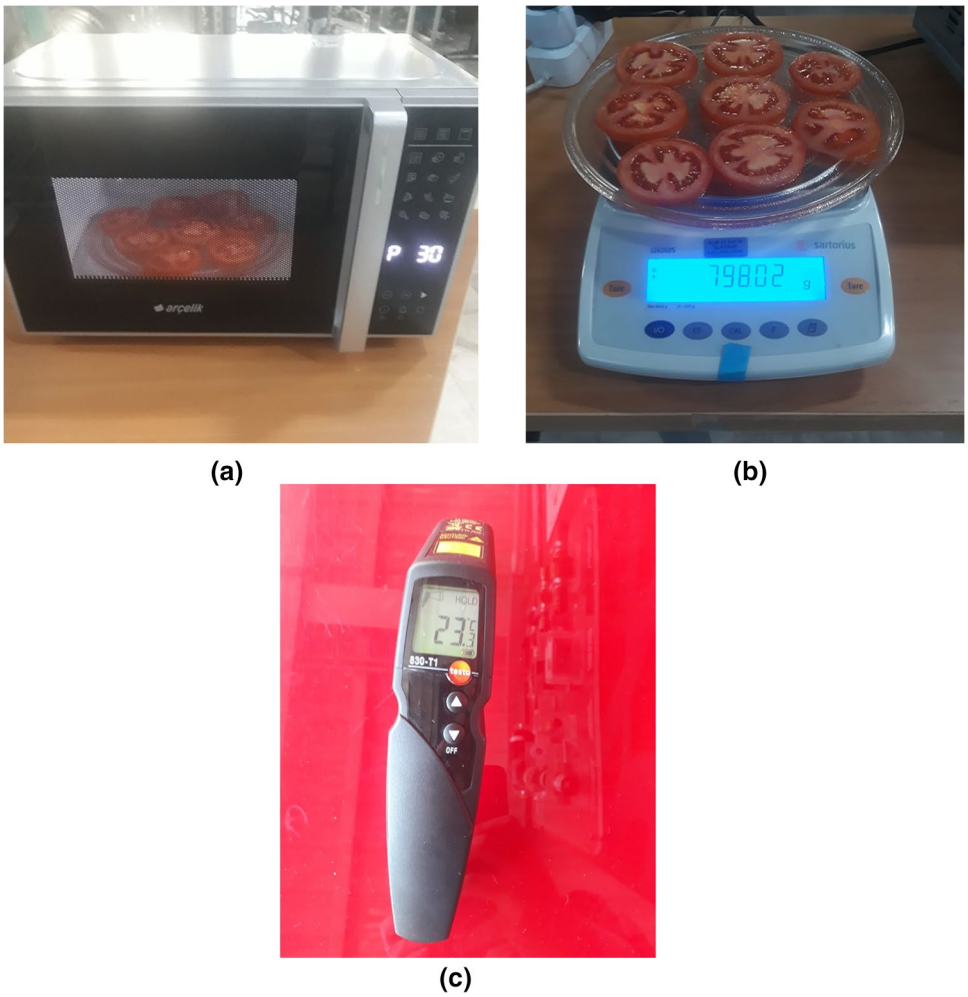


Fig. 2 Experimental setup **a** microwave oven, **b** electronic analytical and precision balance, **c** infrared thermometer with laser marking

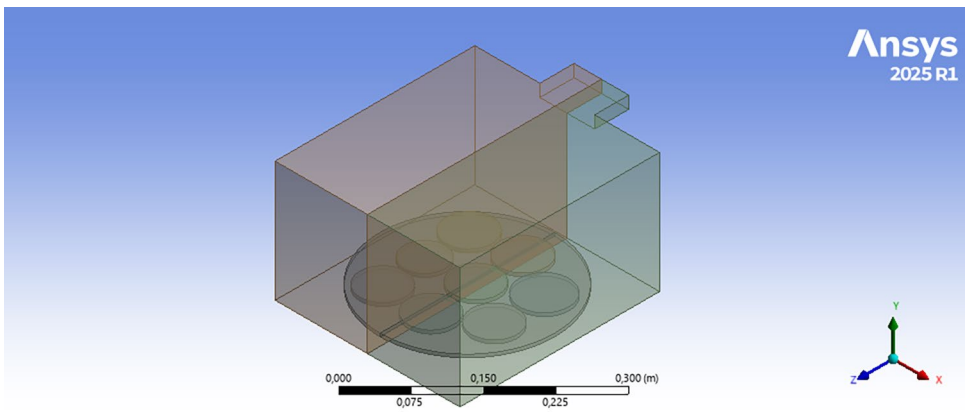


Fig. 3 Geometry of the microwave oven model

ratio (MR) as a function of drying time (t) and are mathematically corresponded to as follows:

Henderson & Pabis model:

$$\mathrm{MR} = a \cdot \exp(-k \cdot t) \tag{6}$$

Fick's diffusion model (first-term approximation):

$$\mathrm{MR} = \frac{8}{\pi^2} \cdot \exp(-k \cdot t) \tag{7}$$

Table 2 Tomato's thermophysical and electromagnetic properties that were employed in the CFD calculations

Temperature/°C	Density/gcm^{-3}	Thermal conductivity/Wm^{-1} K^{-1}	Specific heat/ Jg^{-1} K^{-1}	Relative permittivity/-	Electrical conductivity/ Sm^{-1}
0	1.050	0.56	3.90	71.5	0.30
10	1.045	0.55	3.92	69.7	0.42
20	1.040	0.54	3.95	67.8	0.54
30	1.034	0.53	3.98	66.1	0.66
40	1.028	0.52	4.02	64.3	0.78
50	1.020	0.51	4.07	62.5	0.90
60	1.010	0.49	4.12	60.7	1.02
70	1.000	0.47	4.18	58.9	1.14
80	0.990	0.45	4.25	57.0	1.26
90	0.980	0.43	4.33	55.2	1.38
100	0.970	0.41	4.42	53.4	1.50

Page model:

$$\mathrm{MR} = \exp(-k \cdot t^{n}) \tag{8}$$

Wang & Singh model:

$$\mathrm{MR} = 1 + a \cdot t + b \cdot t^{2} \tag{9}$$

For each model, the *curve_fit* function from the SciPy library was utilized to accomplish the nonlinear regression analysis in Python. It estimates the model parameters utilizing a nonlinear least squares fitting technique. The fitting process involved approximating the model parameters a, k, n, b for each model by minimizing the differences between the experimental and expected MR values. To assess each model's goodness of fit, the following statistical methods were computed:

Coefficient of determination (R^2):

$$R^2 = 1 - \frac{\sum(\mathrm{MR}_{\mathrm{exp}} - \mathrm{MR}_{\mathrm{pred}})^2}{\sum(\mathrm{MR}_{\mathrm{exp}} - \overline{\mathrm{MR}}_{\mathrm{exp}})^2} \tag{10}$$

Root Mean Square Error (RMSE):

$$\mathrm{RMSE} = \sqrt{\frac{1}{N}\sum_{i=1}^{N}.(\mathrm{MR}_{\mathrm{exp,i}} - \mathrm{MR}_{\mathrm{pred,i}})^2} \tag{11}$$

where $\mathrm{MR}_{\mathrm{exp}}$ and $\mathrm{MR}_{\mathrm{pred}}$ are the experimental and model-predicted moisture ratios, respectively, and N is the number of experimental data points. In these equations, also a, b, n are empirical constants, and k is the drying rate constant.

The model with the highest R^2 value and the lowest RMSE was considered to give the best representation of the experimental drying data.

Results and discussion

Numerical analysis of the temperature distribution and effect of power

Figure 6 illustrates the transient temperature distribution within product slices after 45s of microwave drying at two power levels: 210W (a) and 350W (b).

Ansys transient thermal analysis was utilized to run the simulation, which shed light on the spatial thermal gradients that form under changeable energy conditions.

At 210W, with the highest recorded temperature of roughly 63.5 °C on the right side of the tray, the temperature distribution is comparatively uniform, as seen in Fig. 6. This reduces the possibility of localized overheating by indicating a more uniform and moderate heating process. Because of the slower temperature response, which may promote quality retention by lowering thermal deterioration, most of the product mass stays within the 20–50 °C range.

On the contrary, a much greater maximum temperature of roughly 90.8 °C and a wider temperature gradient across the slices are shown by the simulation at 350W. Areas that get much hotter, called "hot spots," stand out more in this case. That uneven heating is a common problem in microwave

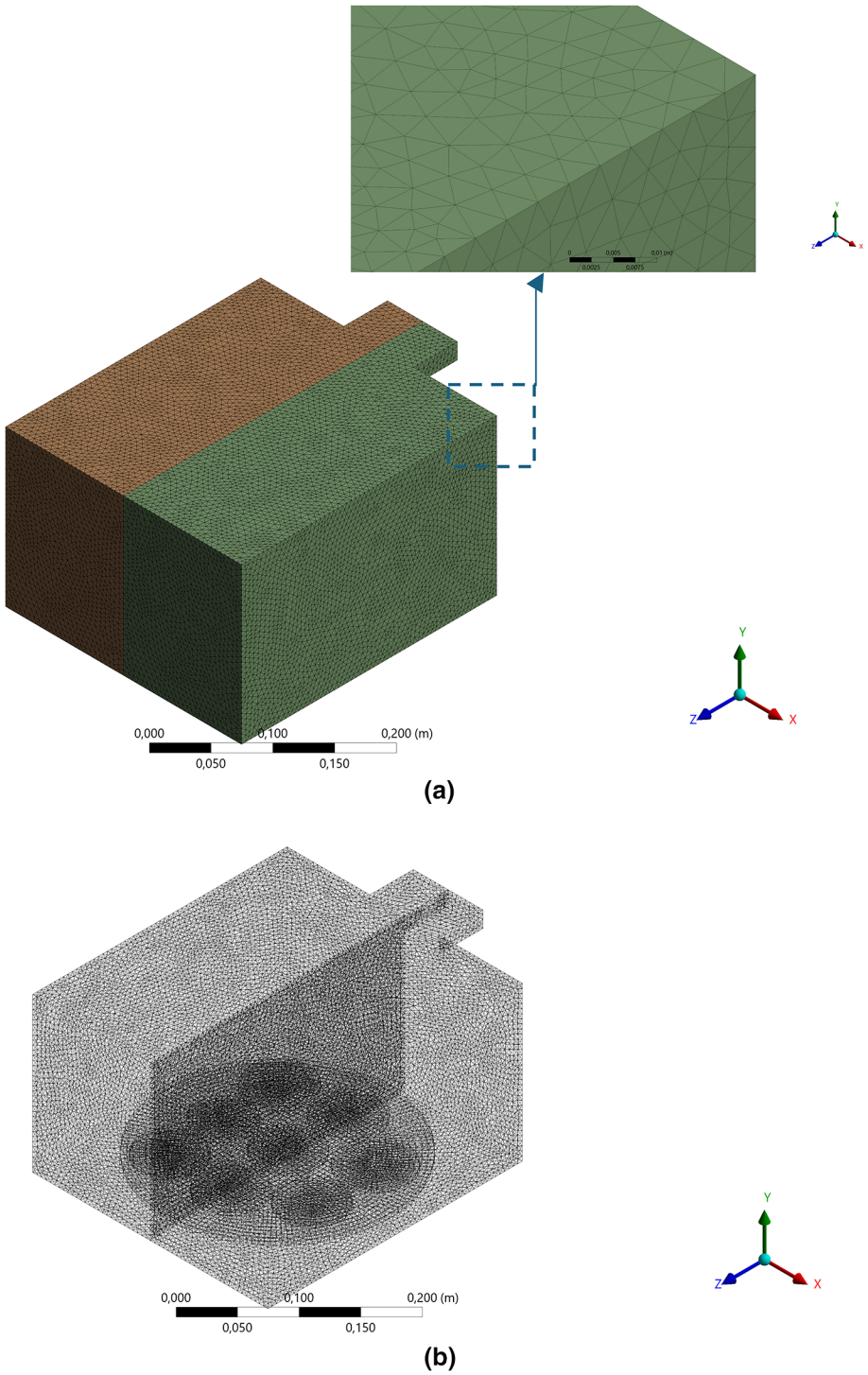


Fig. 4 **a** Mesh element, **b** mesh element wire frame

drying, as highlighted in some literature studies [9, 38, 39]. It occurs mostly due to the material's dielectric characteristics and interference patterns. To mitigate hot spots, recent studies have emphasized the role of sample configuration, density, and morphology; for instance, Shen et al. [38] demonstrate that gap sensitivity and shape selectivity are decisive factors in hot spot evolution. Specifically, it was reported that even a minimal increase in the gap between samples (e.g., 0.8 mm) can significantly inhibit focused hot spots by suppressing evanescent waves at the boundaries. These findings suggest that the temperature distributions observed in Fig. 6 could be further optimized by controlling the spatial arrangement and geometry of the food slices to prevent resonance-induced thermal runaway.

Fig. 5 Mesh quality assessment

Quality	
Check Mesh Quality	Yes, Errors
Target Skewness	Default (0,9)
Smoothing	Medium
Mesh Metric	Element Quality
Min	0,26019
Max	0,99964
Average	0,83863
Standard Deviation	9,4839e-002

Quality	
Check Mesh Quality	Yes, Errors
Target Skewness	Default (0,9)
Smoothing	Medium
Mesh Metric	Skewness
Min	1,3057e-010
Max	0,79098
Average	0,22539
Standard Deviation	0,11867

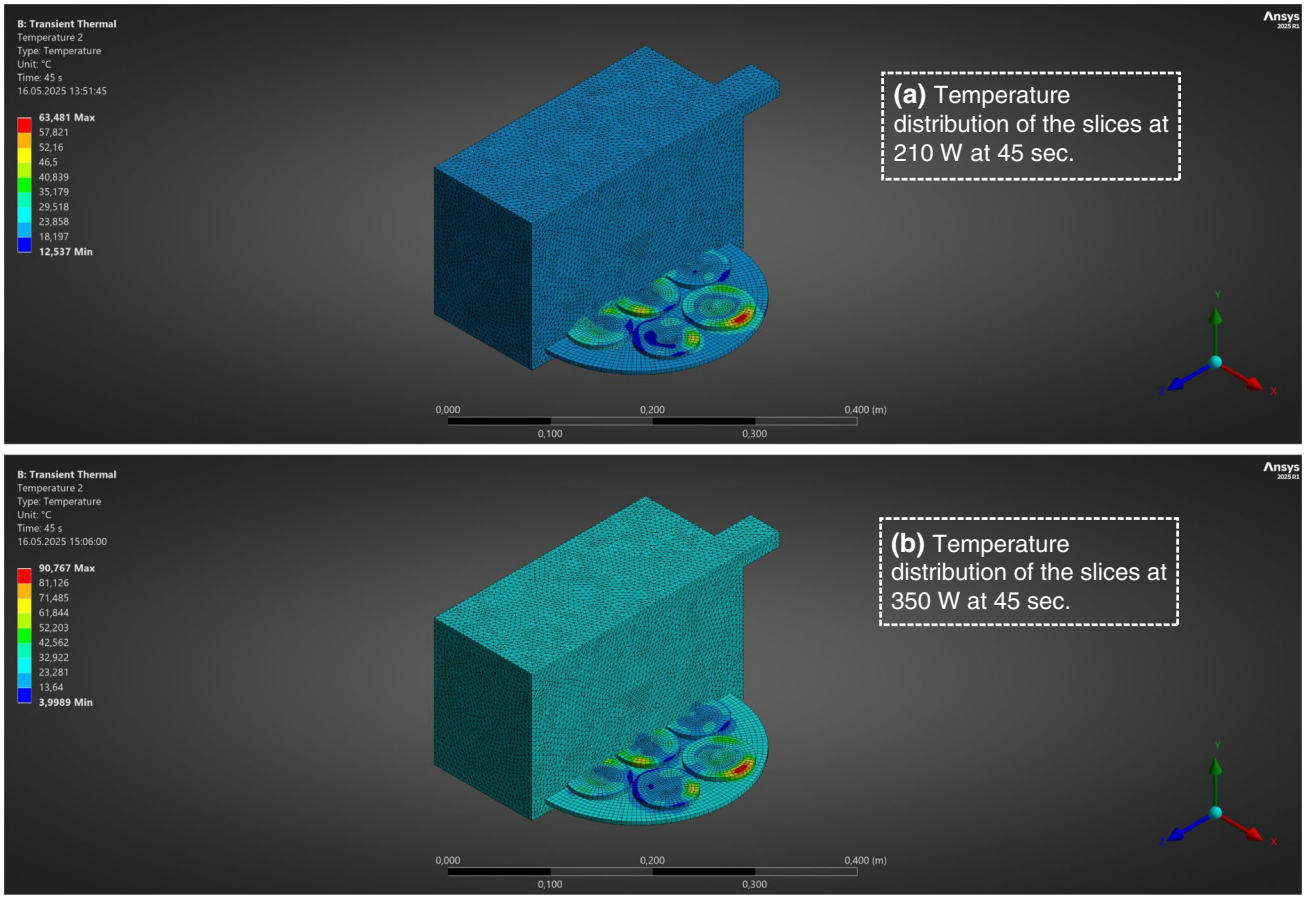


Fig. 6 Temperature distribution of the tomato slice in the microwave at 45s **a** 210W power level, **b** 350W power level

The temperature changes over time in food slices on a circular tray when exposed to microwave heating at 210 and 350W is shown in Fig. 7.

Figure 7 displays the temperature changes over time in food slices on a circular tray when exposed to microwave heating at 210W (a) and 350W (b) for 30s, utilizing Ansys transient thermal analysis.

In 210W case, with a maximum temperature of roughly 89.9 °C, the slices heat up moderately. With most of the slices falling between 30 and 65 °C, the temperature distribution seems to be rather uniform. Because it prevents the development of temperature gradients that might cause uneven drying or product deterioration, this homogeneity is preferred in microwave drying processes.

However, in the 350W case, the thermal dynamics change dramatically, with maximum surface temperatures reaching 134.5 °C within a small localized region. This significant rise is coupled with increased thermal

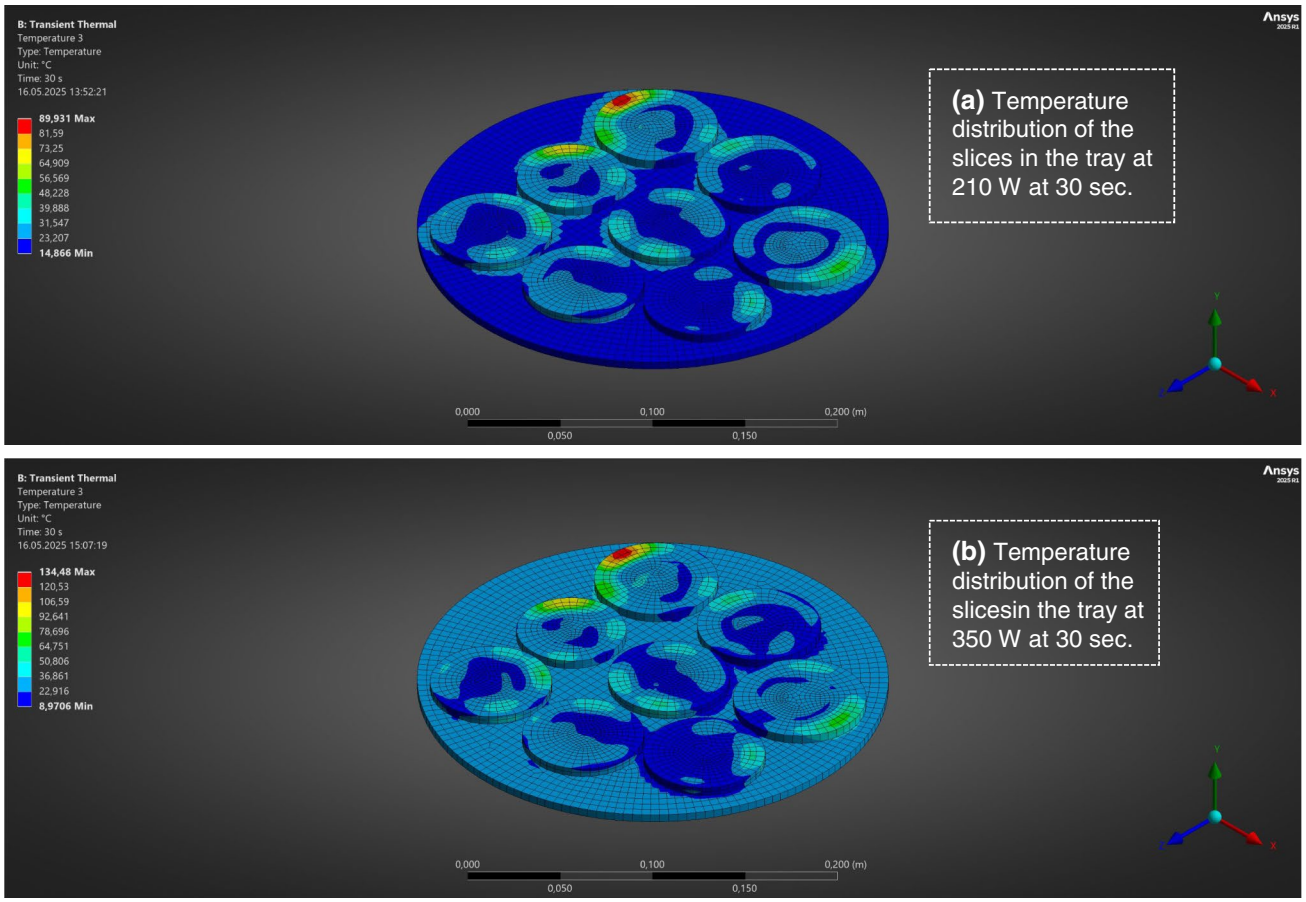


Fig. 7 Temperature distribution of tomato slices on a circular tray under microwave at 30s for two different power levels **a** 210W power, **b** 350W power

heterogeneity, as shown by the presence of noticeable "hot spots" in several slices, especially those close to the tray's edge. These hot spots occur because microwaves do not heat uniformly throughout the cavity—they create interference patterns and uneven energy distribution, which are common problems in microwave drying. The development of hot spots during microwave drying is a complex phenomenon that has been linked to a number of variables in the literature [40, 41]. Too much MW power can lead to localized overheating; a higher loading density can produce more uniform heating, while a lower density can produce hot spots inside food. Unevenly sliced vegetables and other items with unusual shapes or thicknesses may heat less evenly, creating hot areas [41]. These factors likely contribute to the peak temperatures observed at 350W, where electromagnetic interference patterns become more pronounced. Most of the slice temperatures fell between 30 and 78 °C, which is consistent with the anticipated thermal behavior. In a similar study involving the microwave drying of high-moisture Trabzon persimmons, temperature values within a range of 18–93.1 °C were recorded at 350W power [42].

The temperature distribution of the center slice placed on the tray is displayed in Fig. 8.

Figure 8 displays the temperature distribution of the center slice placed on the tray after 30s of exposure.

At 210W, with a highest recorded maximum temperature of roughly 43.08 °C and showing a balanced temperature gradient, in the center slice at that power level, most of the slice stays between 20 and 40 °C, and hot spots have not occurred. This could help maintain the microstructure of tomatoes that are sensitive to overheating.

In contrast to the 350W case, the highest temperature of approximately 58.45 °C was observed, along with a further uneven temperature distribution and gradient. A more uneven distribution is seen on the temperature map, which is indicative of higher power levels brought on by more intense dielectric heating. Thermal hot spots which are around the slice show non-uniform internal energy absorption.

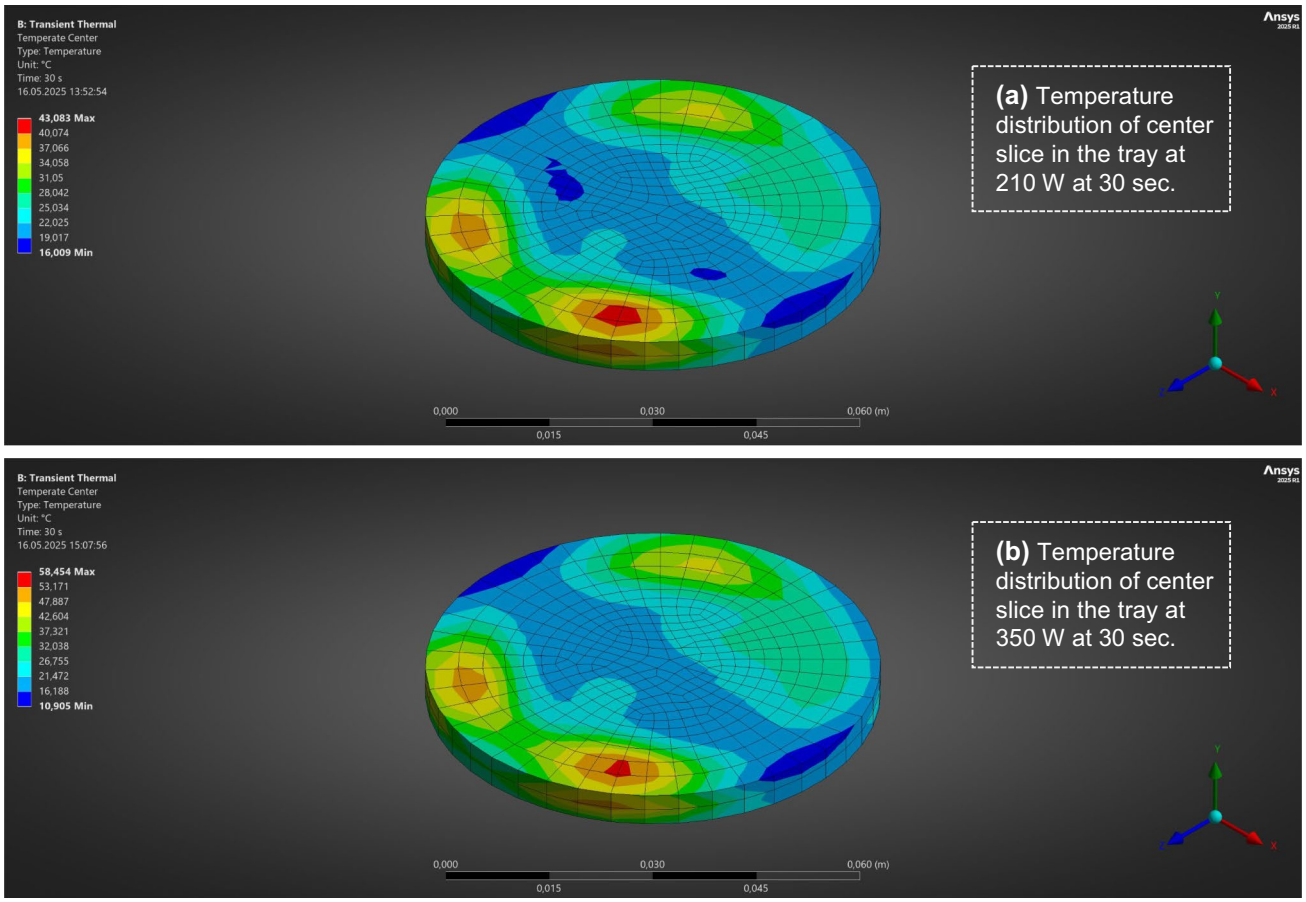


Fig. 8 Temperature distribution of the center tomato slice on a circular tray under microwave at 30s for two different power levels **a** 210W, **b** 350W

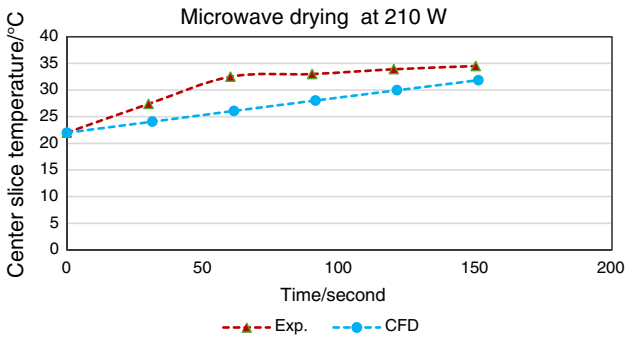


Fig. 9 Validation of temperature of the center slice with experimental data for 210W power

Validating the model with experimental results and mean absolute error (MAE) analysis

The measured center slice temperature is compared with the average temperature of the center slice in CFD data. The mean absolute error (MAE) between experimental results and the CFD data is shown in this section. The experimental and CFD center slice temperature profiles at 210W are presented in Fig. 9.

Figure 9 shows the temperature variation at the center slice of the tomato slice during microwave drying at a power level of 210W. The product's heat absorption behavior is demonstrated by the rising temperature trend over time indicated by both experimental and CFD (computational fluid dynamics) data. However, CFD predictions consistently fall below the experimentally measured temperatures. The mean absolute error (MAE) between the experimental and CFD data was calculated to be roughly 3.55 °C. This discrepancy could have multiple causes; the laser marked infrared thermometer, which measures temperature, has a fixed emissivity value. But the emissivity of tomatoes depends on the temperature. There may be a reason for that little discrepancy. It is possible that the simulation environment did not accurately depict the microwave power distribution. Discrepancy may also be caused by surface effects in the experimental setup and measurement uncertainties.

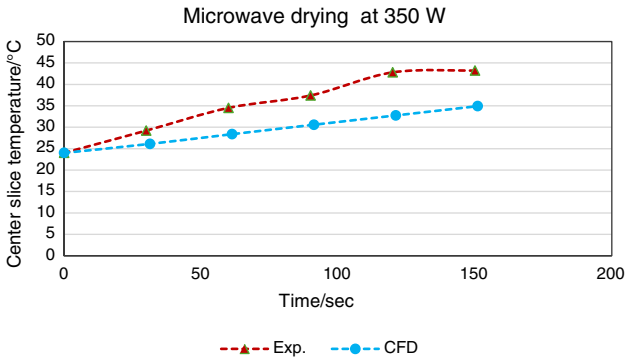


Fig. 10 Validation of temperature of the center slice with experimental data for 350W power

Generally, there is good consensus between the two datasets despite the quantitative discrepancies. This suggests that the thermal behavior during microwave drying can be correctly predicted by the CFD model.

The experimental and CFD center slice temperature profiles at 350W are presented in Fig. 10.

Comparing experimental results and CFD, Fig. 10 shows the average temperature of the center slice in CFD and the center slice point in experimental temperature during microwave drying at 350W. Over time, both datasets show a consistent increase in temperature.

But the experimental temperatures are routinely underestimated by the CFD model, particularly after 60s. The datasets' mean absolute error (MAE) is roughly 5.73 °C, which indicates a notable departure from actual behavior when power input is increased. This notable departure can be attributed to the same reasons for the above-mentioned in the case 210W, as well as to the following.

Higher microwave power levels, like 350W, cause a more noticeable discrepancy between CFD projections and experimental evidence. Numerous related physical and modeling elements are to blame for this.

At low power, minor inaccuracies in microwave energy distribution have minimal impact on temperature predictions. However, at higher power, intense hot spots and uneven heating make modeling more challenging. Most CFD models assume uniform energy absorption, often underestimating localized heating effects. It is considered that intense hot spots and nonlinear heating effects pose significant challenges for accurate simulation modeling; consequently, these factors increase the mean absolute error in this study. The material's surface heats up rapidly than its interior. This discrepancy becomes exaggerated with high power. In the literature, experimental values for numerical models of microwave drying have been compared with simulation results, and similar error ranges have been obtained with this study. For instance, Wang et al. [43] reported the root mean square errors were 3.44 °C for temperature predictions in a numerical study on wheat bran. In addition, Zhang et al. [44] reported a maximum root mean square error (RMSE) of 3.33 °C for the temperature of Zanthoxylum bungeanum during microwave drying. Yan et al. [45] implemented and validated a 3D coupled electromagnetic-heat and mass transfer model for the vacuum microwave drying (VMD) of pineapple slices. The model demonstrated strong predictive accuracy, with mean absolute errors (MAE) of 2.478% for moisture content and 2.791 °C for surface temperature. These reported values are in good consistent with the error margins observed in this study, further validating the reliability of the numerical model.

Drying kinetics

In this section, moisture content of the tomato slices through the microwave drying process has been calculated utilizing different mathematical models and experimental results. Experimental results and predicted moisture ratios using Henderson–Pabis, Page, Wang & Singh, and Fick models are shown in Fig. 11.

Four popular drying models—three thin-layer models (Henderson–Pabis, Page, and Wang & Singh) and Fick's diffusion model—are compared with experimental data for tomato slices (5 mm thick) that were dried at 210W microwave power in Fig. 11. The findings demonstrate that the Wang & Singh ($R^2 = 0.991$) and Page ($R^2 = 0.994$) models provide a good fit to the experimental data, the poor performance of the Fick model was observed with the coefficient of determination ($R^2 = 0.742$) as shown in Table 3, and this result is considered rational, given that microwave drying involves non-uniform heating and complex moisture diffusion mechanisms. In the experimental stage, drying was conducted at a moderate microwave power level (210W) for a total duration of approximately 78 min. This power setting was carefully chosen to prevent instant overheating and preserve product quality. To assurance product stability during storage, the ultimate moisture level of tomato was lowered to approximately 5–6% (wet basis). The first-term approximation of the analytical solution of Fick's second law, which is mostly applicable during the mid—to late phases of drying, was utilized to match the Fick's model. The fitting performance of the mathematical models at 210W is presented in Table 3.

Experimental results and predicted moisture ratios using Henderson–Pabis, Page, Wang & Singh, and Fick models are shown in Fig. 12.

In this case, the same four models are fitted to the experimental data for 350W power level as depicted Fig. 12. Both the Page and Wang & Singh models showed outstanding agreement with the experimental data, each achieving a high coefficient of determination ($R^2 = 0.995$ and $R^2 = 0.981$)

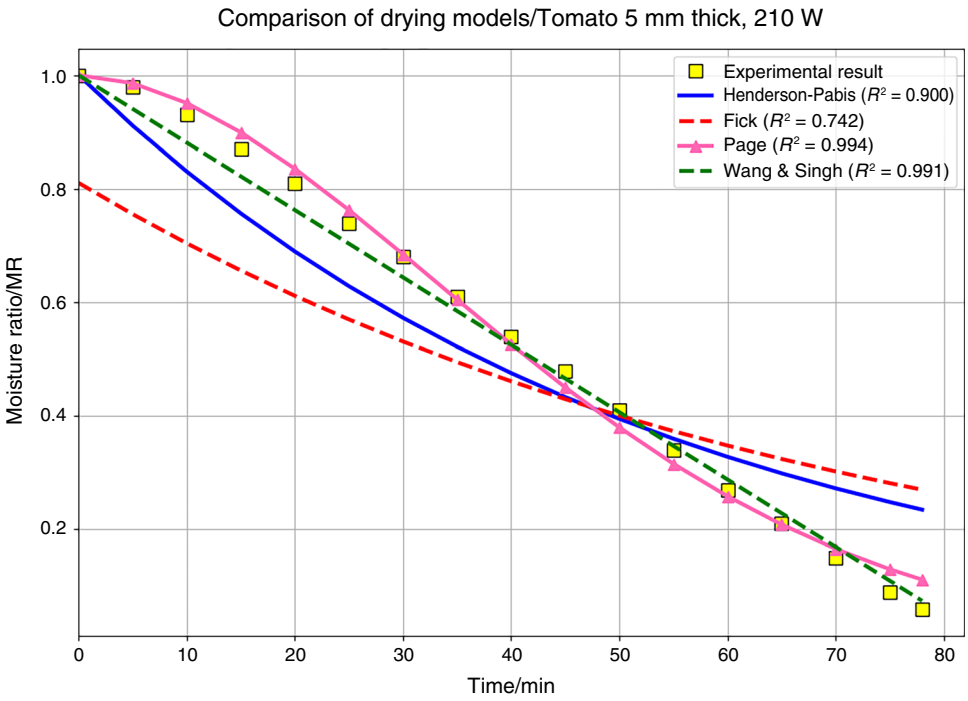


Fig. 11 Drying models and experimental data at 210W power level

Table 3 The fitting results of the models for 210W power level

Models	*k*	*n*	*a*	*b*	R^2	RMSE
Henderson–Pabis	0.01858359	–	1.00001	–	0.9004	0.0977
Page model	0.00073179565	1.83735046	–	–	0.9940	0.0240
Wang & Singh	–	–	− 0.0118681911	1.01498103e–16	0.9915	0.0286
Fick's diffusion model	0.01410147	–	–	–	0.7425	0.1572

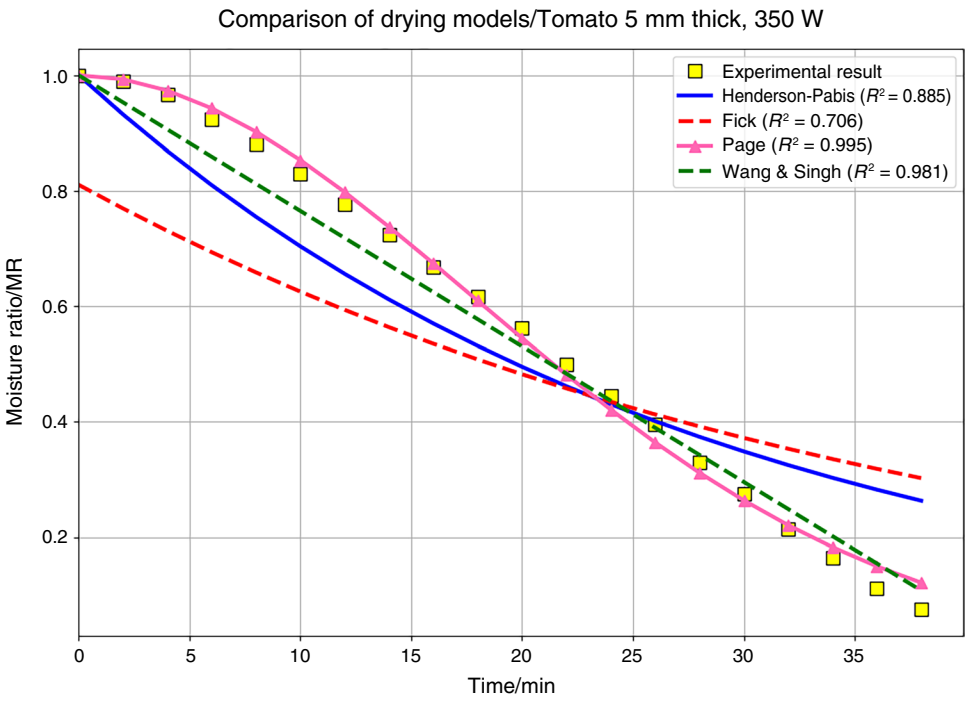


Fig. 12 Drying models and experimental data at 350W power level

Table 4 The fitting results of the models for 350W power level

Models	*k*	*n*	*a*	*b*	R^2	RMSE
Henderson–Pabis	0.03511554	–	1.00001	–	0.8847	0.1026
Page model	0.00183090492	1.93751345	–	–	0.9953	0.0208
Wang & Singh	–	–	– 0.0234720257	2.84612387e-14	0.9807	0.0419
Fick's diffusion model	0.02594162	–	–	–	0.7058	0.1639

as shown in Table 4. In contrast, the Henderson & Pabis showed a moderate fit ($R^2 = 0.885$), whereas Fick's diffusion model, which failed to accurately depict the drying behavior in this situation, offered the worst fit ($R^2 = 0.706$). Since the Page and Wang & Singh models are more flexible in capturing the nonlinear moisture removal dynamics that are normally seen at higher microwave power levels, they perform better. Also, to ensure product stability while being stored, the tomato's final moisture content was reduced to roughly 4–5% (wet basis) at 350W power level.

These results confirm the notion that, in contrast to simpler analytical models like the Fick diffusion model, empirical and semiempirical models—such as those developed by Page and Wang & Singh—are better suited for simulating the thin-layer microwave drying of tomato slices. A comparative analysis of the mathematical models applied in this study reveals that the Page model is the most effective for predicting drying kinetics. This performance is consistent with findings reported for various products in the literature. For example, Kusuma et al. [46] and Ahmed et al. [47] reported that the Page model provided the best fit to experimental drying data. This superior performance is mainly attributed to its capability to capture the nonlinear drying behavior that simpler models often fail to represent. Such capability is particularly important in microwave drying, where moisture removal typically occurs at a variable rather than constant rate. The empirical exponent *(n)* included in the Page model enables it to better adapt to these nonlinear drying dynamics, resulting in more accurate predictions of moisture ratio over time.

The Fick model, grounded in the analytical solution of Fick's second law of diffusion, exhibits the lowest determination coefficients ($R^2 = 0.742$ at 210W and $R^2 = 0.706$ at 350W) among the tested models, indicating a poor fit to the empirical data. For the most part of the drying process, especially in the middle to late phases, this model tends to underestimate the moisture ratio. The Fick model is a theoretical model and is basically based on pure diffusion. Its oversimplified assumptions, such as constant effective diffusivity and infinite slab geometry, which fall short in capturing the complex moisture migration mechanisms under microwave drying, are likely the cause of this disagreement. Unlike convective drying, microwave-assisted processes involve non-uniform internal heating and varying moisture gradients, which violate the assumptions of the classical diffusion-based model. In addition, moisture transport in microwave drying may occur not only by diffusion but also in a "forced:" form due to vapor pressure difference and local heating. The Fick model is inadequate to explain this rapid and irregular moisture transport. Hence, the Fick model lacks the flexibility required to describe the nonlinear and spatially changing drying behavior observed in this study. Therefore, the low R^2 value and poor fit of the model occur. Despite this, Fick's second law remains the standard mathematical framework for determining the effective moisture diffusivity (*Deff*), a critical parameter for characterizing the internal resistance to moisture transport. This approach has been extensively utilized in microwave drying studies to evaluate the diffusion kinetics of various agricultural products [42, 48].

The Wang & Singh and Page models are empirical models mainly focused on experimental data fitting. Based on experimental results, these models were created to directly depict the time-dependent variation in moisture content that occurs through the drying process. They seek to precisely depict the observed drying behavior numerically rather than trying to fully explain intricate physical mechanisms. In microwave drying, sometimes energy and heat distribution can be highly non-uniform, often resulting in the formation of hot spots and exhibiting moisture transport complexities that exceed classical diffusion principles. Extensive research indicates that the Page and Wang & Singh models consistently yield higher R^2 and lower sum of squared errors (SSE) values compared to other models, proving suitable in optimizing drying parameters and achieving uniform moisture distribution. For instance, Tian et al. [48] employed the Page, Lewis, Quadratic, and Wang & Singh models to evaluate the fit of hydration ratio data for zinc leach slag. According to the results, the Page model was identified as the most suitable model for describing the drying kinetics. Additionally, the Wang & Singh model also demonstrated strong performance, achieving a high coefficient of determination ($R^2 = 0.93963$) and a low residual sum of squares (RSS = 0.08428). Also, Khatun et al. [49] al. investigated the drying kinetics of dragon fruit slices utilizing a microwave-vacuum dryer. Their findings revealed that the Wang and Singh model was the most suitable, demonstrating high R^2 and low RMSE values, thereby providing accurate insights

into the drying process. These studies demonstrate that the Page and Wang & Singh models consistently yield high predictive accuracy in the literature. Similarly, in the present study, these models provided the best fit to the experimental data, confirming their reliability.

Thanks to their flexible formulations, the Wang & Singh and Page models can effectively capture these irregularities and complex phenomena, such as the rapid water evaporation induced by microwave energy. The fitting performance of the mathematical models at 350W is presented in Table 4.

Electric field

Sample volume, microwave frequency, and dielectric characteristics all influence how the electric field is distributed during microwave heating [50, 51]. Figure 13 illustrates how the electric field primarily appears in the majority of the tomato slices, particularly water in the slices. Thermal energy in water is mostly absorbed from the electric field, specifically from microwaves. The findings, which were obtained from Ansys Electronics Desktop simulations, provided light on the microwave energy's spatial distribution and absorption inside the sample region. The electric field distribution and volume loss density of the tomato slices are depicted in Fig. 13.

Peak volume loss density is 1.57×10^7 Wm^{-3} at 210W, and the maximum electric field magnitude is approximately 19,946 Vm^{-1}, as shown in Fig. 13. The E-field distribution illustrates moderate field localization near the border of the cylindrical samples, indicating partial energy penetration and relatively uniform exposure across the load cross section. In line with this, the volume loss density map shows somewhat irregular power absorption, with higher energy dissipation close to the edges. The electric field distribution exhibits localized intensities at the edges of the samples, a phenomenon widely recognized in the literature as the "edge effect." These high-energy regions, or hot spots, are consistent with the electromagnetic modeling of dielectric materials reported in similar drying studies [44, 52].

In contrast, increasing the input power level to 350W increases the electric field, reaching a maximum of 24,202 Vm^{-1}, with the volume loss density peaking at 2.63×10^7 Wm^{-3}. The results showed that the electric field strength increased when the microwave power increased because more energy was generated, as previously reported in the literature [53]. However, a high E-field can lead to more uneven heating, causing hot and cold spots due to standing waves and complex interactions with the drying product. This uneven heating is visibly shown in the volume loss density plots, where sharp differences between nearby areas highlight the risk of thermal non-uniformity at higher

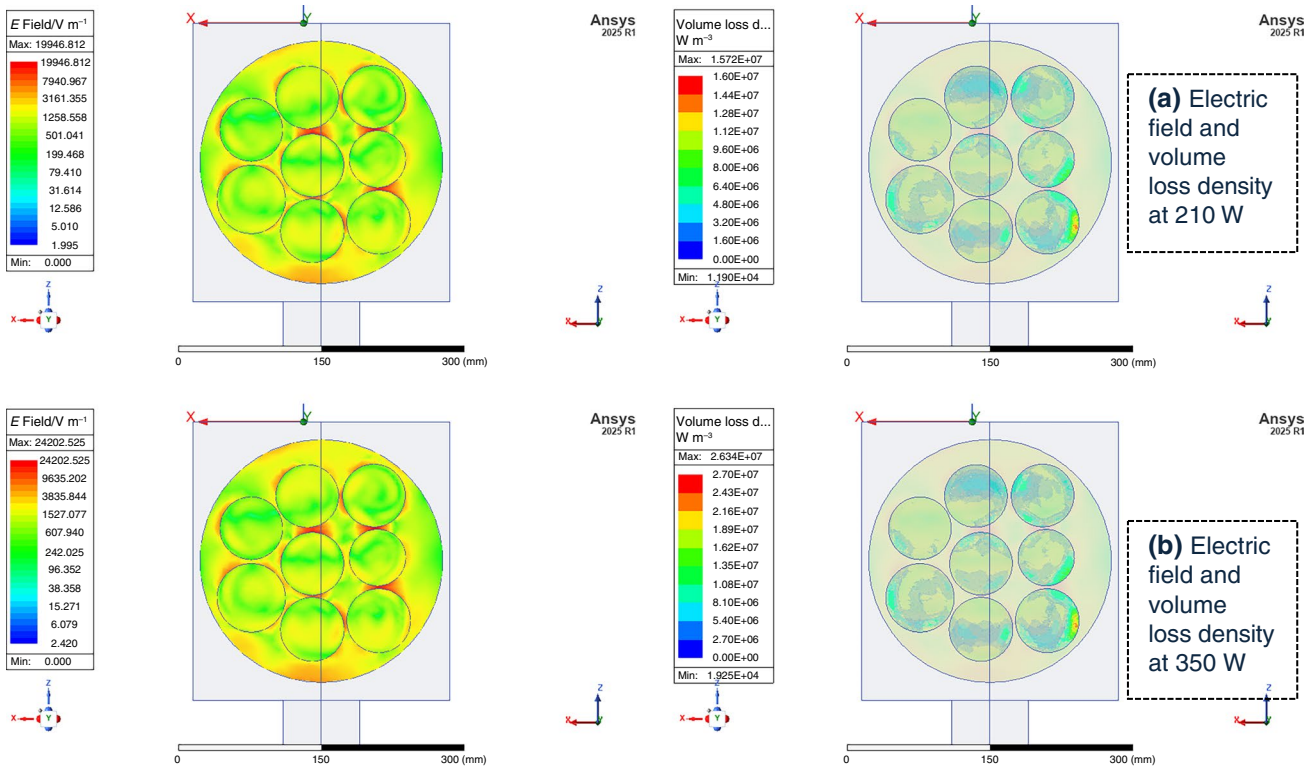


Fig. 13 Electric field and volume loss density distribution for two power levels **a** 210W, **b** 350W

power. These results demonstrate that it is challenging to get even heating with microwaves, remarkably at high power where the electric field changes a lot in different areas. It also highlights how important it is to arrange the sample well and design the chamber properly to avoid hot spots and get uniform drying.

Future trends and challenges of the topic

Computational fluid dynamics (CFD) is a powerful instrument for simulating the microwave drying process. Nonetheless, there are several challenges to model all processes in truly predictive and scalable models. The main challenges in precise simulating microwave drying processes arise from the dynamic characteristics of the materials being dried as well as the intricate, related nature of the phenomena involved. A big challenge is that microwave drying involves multiple processes at once. These include the spread of electromagnetic waves (described by Maxwell's equations), heat transfer, moisture movement, and sometimes material shrinkage causing deformation. All these are required to be solved together. Owing to the inherent complexity of these coupled processes, existing models have undergone several approximations and simplifications, which often decrease their forecast precision and practical application. The process of accurately connecting these occurrences is still difficult and computationally intensive.

Another challenge is related to changing material properties, as the moisture level falls during the drying process, the material's dielectric characteristics, thermal conductivity, and porosity all undergo substantial changes. It is tough to accurately incorporate these dynamic property changes into CFD models. Also, particularly for complex food products and composite materials, the databases currently available for these qualities are either lacking or inconsistent. The dielectric constant, thermal conductivity, specific heat, mass diffusivity, and other temperature and moisture-dependent characteristics must be exactly understood to ensure accurate CFD modeling.

Most CFD models available today are only suitable for laboratory-scale applications and simplified geometries. It is computationally costly to sufficiently model the complex cavity geometries, multiple magnetrons, and irregular product forms that are often found in industrial microwave dryers.

A common obstacle still exists in the limited availability of comprehensive experimental data for model validation. Comprehensive validation of CFD predictions is limited by the challenge of monitoring internal temperature and moisture distributions during microwave drying. Being able to accurately monitor temperature and moisture changes of products throughout the microwave drying process is a challenge that researchers often face.

Microwave drying CFD models involve multiple physical processes and require high computational power. Resolving electromagnetic waves while also simulating heat and mass transfer at different scales builds an extreme load that borders their usage in practical applications.

Creating dependable numerical algorithms that can manage the significant interaction between thermal, mass transfer, and electromagnetic processes should be the fundamental objective of future study. Several promising approaches are proposed, including:

Machine learning-enhanced coupling algorithms that can predict optimal solution strategies can be utilized; machine learning algorithms can perform optimizations that enable simultaneous multiphysics processes to reach their conclusions with fewer operations. Utilization of these algorithms can reduce simulation time, allowing for real-time process management and monitoring.

To effectively resolve sharp spatial gradients in the electromagnetic field, particularly close to material interfaces and boundary layers, future studies should discover the application of adaptive mesh refinement approaches. In areas of high field intensity, adaptive mesh refinement can improve solution accuracy by constantly fine-tuning the computational grid without having to pay the excessive computational expenses of uniformly fine meshes. Additionally, to properly represent actual drying behavior, future models should incorporate dynamic material properties, like specific heat, thermal conductivity, and dielectric constants that vary with temperature and moisture.

Conclusions

In this study, a numerical model was created, and the temperature distribution and hot spots of the product in the microwave drying processes at different power levels were monitored thanks to the created model. The temperature values obtained from the CFD simulation were compared with the temperatures acquired from the experimental consequences, and the results were evaluated. The difference between the two power levels in the CFD simulations shows a clear trade-off: More energy accelerates the drying process. But it makes heat spread unevenly. That can harm the product's quality and nutrients. Electric field distributions were examined to identify locations of intense thermal energy absorption. Four well-known drying models—Fick's diffusion model, Wang & Singh, Page, and Henderson–Pabis—are fitted to the empirical data of tomato slices. Coefficient of determination (R^2) and root mean square error (RMSE) statistical methods were utilized to evaluate the suitability of these models.

These important points were made from the results:

- In lower power level (210W), the temperature distribution of the slices is uniform, and no areas of extremely high temperature were observed, as concluded from numerical results. Most of the slices' temperatures fell between 30 and 65 °C, conversely in 350W power level, a hot point region occurred in the slices, and at this power level, most of the slices' temperatures were around 30 and 78 °C. The occurrence of hot spots reflects a non-uniform distribution of the electromagnetic (EM) field, causing certain regions to absorb more energy and heat up faster, which is an undesirable phenomenon in the drying process.
- The average center temperatures of the tomato slices coming from CFD results were contrasted with the experimental data. In 210W power level, it was found that the mean absolute error (MAE) between the experimental and CFD data was around 3.55 °C. In 350W, the mean absolute error (MAE) of the datasets is around 5.73 °C. In lower power level, the experimental and CFD results are consistent and close to each other. This shows that the proposed model is accurate and can be utilized to reduce the number of experimental tests to be performed. However, there was a more pronounced difference between CFD predictions and experimental data at the higher microwave power level (350W). This phenomenon is likely attributed to localized hot spots, nonlinear heating effects, and rapidly changing thermal energy transfer at the higher power level. Nevertheless, our MAE value is still at an acceptable level at 350W power level.
- Four commonly used drying models were applied and compared with the experimental results. Utilized models are these: Henderson–Pabis, Page, Wang & Singh, and Fick's diffusion model. The Page and Wang & Singh showed outstanding performance at both 210 and 350W power levels. The worst fit was provided by Fick's diffusion model, which was unable to adequately represent the drying behavior in two power levels. This difference is possibly due to its oversimplified assumptions, which fail to capture the intricate moisture migration mechanisms under microwave drying. These assumptions include constant effective diffusivity and infinite slab geometry. Pure diffusion is essentially the foundation of the theoretical Fick model.
- In microwave drying, moisture may be transported not only by diffusion but also in a "forced" form because of local heating and vapor pressure differences. This quick and erratic moisture transfer cannot be explained by the Fick model. This approach is commonly used to estimate the diffusion coefficient in literature.
- Empirical models like Wang & Singh and Page use simple equations to fit experimental drying data, making them well-suited for the complexities of microwave drying. Unlike models based on physical mechanisms, their flexibility can account for non-uniformities like hot spots and the rapid moisture evaporation characteristic of microwave heating.
- In microwave drying studies, it is still a noteworthy challenge to capture the temperature and humidity inside the microwave oven with an accurate measurement. These parameters are necessary for verification in CFD studies. In addition, other challenges that researchers frequently confront and future trends of the subject were mentioned.

Acknowledgements The authors would like to acknowledge that this paper is submitted in partial fulfillment of the requirements for the Ph.D. degree at Yildiz Technical University. This study has been financially supported by Yildiz Technical University Scientific Research Projects Coordination Department, Project Numbers: FDK-2022-5199 and FCD-2022-5058.

Author contribution The contribution of each author can be seen below: Emre Arpaci, Ş. Özgür Atayılmaz, Zafer Gemici, and Hakan Demir were involved in conceptualization.

Funding Open access funding provided by the Scientific and Technological Research Council of Türkiye (TÜBİTAK). This work was supported by the Yildiz Technical University Scientific Research Projects Coordination Department (FDK-2022-5199 and FCD-2022-5058).

Data availability No datasets were generated in this study.

Declarations

Conflict of interest The authors declare no conflict of interests.

Ethical approval Not applicable.

Open Access This article is licensed under a Creative Commons Attribution 4.0 International License, which permits use, sharing, adaptation, distribution and reproduction in any medium or format, as long as you give appropriate credit to the original author(s) and the source, provide a link to the Creative Commons licence, and indicate if changes were made. The images or other third party material in this article are included in the article's Creative Commons licence, unless indicated otherwise in a credit line to the material. If material is not included in the article's Creative Commons licence and your intended use is not permitted by statutory regulation or exceeds the permitted use, you will need to obtain permission directly from the copyright holder. To view a copy of this licence, visit http://creativecommons.org/licenses/by/4.0/.

References

1. Shi Y, Cao G, Liu Y, Tao Y, Han Y, Li D. Effect of microwave and hot air drying on the quality of quick-cooking mung bean. Food Mater Res. 2023;3:0–0. https://doi.org/10.48130/FMR-2023-0008.
2. Dehghannya J, Habibi-Ghods M. Moving boundary modeling during drying with intermittent microwave: the effect of pulse ratio. Therm Sci Eng Prog. 2025;63:103745. https://doi.org/10.1016/j.tsep.2025.103745.

3. Härdter N, Geidobler R, Presser I, Winter G. Accelerated production of biopharmaceuticals via microwave-assisted freeze-drying (MFD). Pharmaceutics. 2023;15:1342. https://doi.org/10.3390/pharmaceutics15051342.
4. Ren L, Zhang K, Wang F, Zhang Y, Yang F, Cheng F. Microwave heating of coal slime based on multi-physics field simulations: regulating waveguide port size and sample radius to improve microwave utilization efficiency. Chem Eng J. 2023;470:143975. https://doi.org/10.1016/j.cej.2023.143975.
5. Li B, Fan X, Yu S, Xia H, Nong Y, Bian J, et al. Microwave heating of biomass waste residues for sustainable bioenergy and biomass materials preparation: a parametric simulation study. Energy. 2023;274:127347. https://doi.org/10.1016/j.energy.2023.127347.
6. Predoana L, Atkinson I, Karaj DA, Odhiambo VO, Bakos LP, Nagyné Kovács T, et al. Comparative study of the thermal behavior of Sr–Cu–O gels obtained by sol–gel and microwave-assisted sol–gel method. J Therm Anal Calorim. 2021;143:2893–900. https://doi.org/10.1007/s10973-019-09205-5.
7. Singh D, Singh D, Husain S. Computational analysis of temperature distribution in microwave-heated potatoes. Food Sci Technol Int. 2020;26:465–74. https://doi.org/10.1177/1082013220907434.
8. Khattak HK, Bianucci P, Slepkov AD. Linking plasma formation in grapes to microwave resonances of aqueous dimers. Proc Natl Acad Sci U S A. 2019;116:4000–5. https://doi.org/10.1073/pnas.1818350116.
9. Wang W, Wang B, Sun J, Mao Y, Zhao X, Song Z. Numerical simulation of hot-spot effects in microwave heating due to the existence of strong microwave-absorbing media. RSC Adv. 2016;6:52974–81. https://doi.org/10.1039/C6RA05191J.
10. Bulantekin Ö, Kuşçu A. Evaluation of microwave vacuum drying combined with explosion puffing drying and compared with microwave vacuum drying and hot-air drying by the quality of the dried apple slices. Cogent Food Agric. 2024;10:2404699. https://doi.org/10.1080/23311932.2024.2404699.
11. Tomas-Egea JA, Traffano-Schiffo MV, Castro-Giraldez M, Fito PJ. Hot air and microwave combined drying of potato monitored by infrared thermography. Appl Sci. 2021;11:1730. https://doi.org/10.3390/app11041730.
12. Joardder MUH, Karim MA. Drying kinetics and properties evolution of apple slices under convective and intermittent-MW drying. Therm Sci Eng Prog. 2022;30:101279. https://doi.org/10.1016/j.tsep.2022.101279.
13. Taşova M. Comparison of convective and modified temperature-controlled microwave drying on energy and physicochemical properties of banana slices. J Therm Anal Calorim. 2024;149:14727–39. https://doi.org/10.1007/s10973-024-13805-1.
14. Guemouni S, Mouhoubi K, Brahmi F, Dahmoune F, Belbahi A, Benyoub C, et al. Convective and microwave drying kinetics and modeling of tomato slices, energy consumption, and efficiency. J Food Process Eng. 2022;45:e14113. https://doi.org/10.1111/jfpe.14113.
15. Teleken JT, Dutra AC, Laurindo JB, Carciofi BAM. Numerical modeling of heating tomato pulp in continuous flow microwave-assisted thermal processing: estimation of quality parameters. J Food Process Eng. 2023;46:e14216. https://doi.org/10.1111/jfpe.14216.
16. Jayathunge KGLR, Stratakos ACh, Delgado-Pando G, Koidis A. Thermal and non-thermal processing technologies on intrinsic and extrinsic quality factors of tomato products: a review. J Food Process Preserv. 2019;43:e13901. https://doi.org/10.1111/jfpp.13901.
17. Animashaun OH, Sobowale SS. Microwave exposure of tomato varieties before catalytic oven drying and its effect on physicochemical and bioactive components studied by fourier transform infrared (FTIR) spectroscopy. Food Hum. 2024;2:100197. https://doi.org/10.1016/j.foohum.2023.12.005.
18. Izli N, Isik E. Color and microstructure properties of tomatoes dried by microwave, convective, and microwave-convective methods. Int J Food Prop. 2015;18:241–9. https://doi.org/10.1080/10942912.2013.829492.
19. Qadri OS. Microwave drying of foamed tomato pulp: optimization and mass transfer modelling. Food Process Preser. 2022;46:e15954. https://doi.org/10.1111/jfpp.15954.
20. Hussein JB, Oke MO, Agboola FF, Sanusi MS. Application of soft-computational models for the prediction of some quality traits of microwave-dried tomato slices. Model Earth Syst Environ. 2023;9:567–84. https://doi.org/10.1007/s40808-022-01506-3.
21. Smit P, Van Schoor G, Uren K. A FEM model for microwave absorption and heat transfer in a microwave combination washer dryer. 2013 IEEE International Conference on Industrial Technology (ICIT) [Internet]. Cape Town: IEEE; 2013 [cited 2024 Nov 28]. p. 22–7. https://doi.org/10.1109/ICIT.2013.6505642.
22. Modelling of microwave drying methods for foods. ResearchGate [Internet]. [cited 2024 Nov 29]. https://www.researchgate.net/publication/318381231_Modelling_of_Microwave_Drying_Methods_for_Foods. Accessed 29 Nov 2024.
23. Zhang Z, Qin W, Shi B, Gao J, Zhang S. Modelling of intermittent microwave convective drying: parameter sensitivity. Open Phys. 2017;15:405–19. https://doi.org/10.1515/phys-2017-0045.
24. Schütz S, Di Domenico M, Poretti S, Monleone R. A microwave cavity design and optimisation for a homogeneous and faster drying process inside an industrial Agitated Nutsche Filter. Open Res Eur. 2023;3:63. https://doi.org/10.12688/openreseurope.15520.1.
25. Zhong R, Zheng Q, Yao B, Xiang T. Simulation and Analysis of Efficiency Dielectric Properties of Core-shell Agricultural Products. Nazir MS, Aziz HA, editors. E3S Web Conf. 2021; 257: 01071. https://doi.org/10.1051/e3sconf/202125701071.
26. Ramos PAV, Albuquerque DMS, Pereira JCF. Numerical simulation and optimization of the ceramic pigments production process using microwave heating. Chem Eng Process Process Intensif. 2021;169:108567. https://doi.org/10.1016/j.cep.2021.108567.
27. Tauhiduzzaman M, Hafez I, Bousfield D, Tajvidi M. Modeling microwave heating and drying of lignocellulosic foams through coupled electromagnetic and heat transfer analysis. Processes. 2021;9:2001. https://doi.org/10.3390/pr9112001.
28. Beigi M, Harchegani HB, Torki M, Kaveh M, Szymanek M, Khalife E, et al. Experimental and numerical analysis of thermodynamic performance of microwave dryer of onion. J Food Process Eng. 2022;45:e14116. https://doi.org/10.1111/jfpe.14116.
29. Shen L, Zhu Y, Liu C, Wang L, Liu H, Kamruzzaman M, et al. Modelling of moving drying process and analysis of drying characteristics for germinated brown rice under continuous microwave drying. Biosyst Eng. 2020;195:64–88. https://doi.org/10.1016/j.biosystemseng.2020.05.002.
30. Siddique IJ, Salema AA. Numerical simulation of microwave heating of cylindrical shaped biomass material. SSRN Journal. 2024; https://doi.org/10.2139/ssrn.4875398
31. Hou L, Li R, Wang S, Datta AK. Numerical analysis of heat and mass transfers during intermittent microwave drying of Chinese jujube (*Zizyphus jujuba* Miller). Food Bioprod Process. 2021;129:10–23. https://doi.org/10.1016/j.fbp.2021.06.005.
32. Li B, Feng S, He Q, Zhu Y, Wu J, Yang J, et al. Numerical simulation of continuous microwave drying of rice grains. J Food Process Eng. 2024;47:e14678. https://doi.org/10.1111/jfpe.14678.
33. Choi Y. Effects of temperature and composition on the thermal properties of foods. Transport phenomena. Elsevier Applied Science Publishers; 1986; 99–101.
34. Sosa-Morales ME, Valerio-Junco L, López-Malo A, García HS. Dielectric properties of foods: reported data in the 21st

century and their potential applications. LWT Food Sci Technol. 2010;43:1169–79. https://doi.org/10.1016/j.lwt.2010.03.017.
35. Nelson SO. Dielectric spectroscopy of fresh fruit and vegetable tissues from 10–1800 MHz. J Microw Power Electromagn Energy. 2005;40:31–47. https://doi.org/10.1080/08327823.2005.11688523.
36. Sahin S, Sumnu SG. Physical properties of foods [Internet]. Springer New York; 2006; https://books.google.com.tr/books?id=v854Fu2D7VUC.
37. Yuen FK, Hameed BH. Recent developments in the preparation and regeneration of activated carbons by microwaves. Adv Coll Interface Sci. 2009;149:19–27. https://doi.org/10.1016/j.cis.2008.12.005.
38. Shen L, Zhou J, Zhang X. In situ investigation of the thermal characteristics of microwave resonance-induced focused hotspots in dimers for improving microwave heating uniformity. Case Stud Therm Eng. 2024;54:104052. https://doi.org/10.1016/j.csite.2024.104052.
39. Shen X, Zhao Z, Li H, Tsubaki S, Kishimoto F, Stefanidis GD, et al. A review on the thermometry of microscopic hot spots induced by microwave energy. Renew Sustain Energy Rev. 2026;225:116160. https://doi.org/10.1016/j.rser.2025.116160.
40. Joardder MUH, Karim MA. Toward uniform microwave heating in food drying: principles, technologies, and emerging trends. Food Eng Rev. 2025;17:946–65. https://doi.org/10.1007/s12393-025-09426-5.
41. Shen L, Gao M, Feng S, Ma W, Zhang Y, Liu C, et al. Analysis of heating uniformity considering microwave transmission in stacked bulk of granular materials on a turntable in microwave ovens. J Food Eng. 2022;319:110903. https://doi.org/10.1016/j.jfoodeng.2021.110903.
42. Çelen S. Effect of microwave drying on the drying characteristics, color, microstructure, and thermal properties of Trabzon persimmon. Foods. 2019;8:84. https://doi.org/10.3390/foods8020084.
43. Wang H, Fang B, Chen Y, Ye D, Xie L. Numerical simulation and optimization of microwave drying process of wheat bran. Food Bioprod Process. 2025;151:84–102. https://doi.org/10.1016/j.fbp.2025.03.002.
44. Zhang Y, Du Y, Li Y, He T, Hong T, Gou D, et al. Experimental and numerical study on heat and mass transfer of Zanthoxylum bungeanum microwave drying. Therm Sci Eng Prog. 2025;67:104137. https://doi.org/10.1016/j.tsep.2025.104137.
45. Yan W-M, Zhou Y-S, Qin M, Chen B-L, Li C-H. Enhancing heat and mass transfer uniformity in vacuum microwave drying via turntable rotation and intermittent operation: a case study on pineapple slices. Appl Therm Eng. 2026;292:130351. https://doi.org/10.1016/j.applthermaleng.2026.130351.
46. Kusuma HS, Paradiba H, Wahyuni TD, Amenaghawon AN, El Messaoudi N, Darmokoesoemo H. Comparison of thin-layer drying models for microwave drying of peanuts at varying power levels. Food and Humanity. 2025;5:100754. https://doi.org/10.1016/j.foohum.2025.100754.
47. Ahmed M, Faisal M, Laskar A, Abdullah A, Shahadat M, Umar K, et al. Experimental studies for thin layer model validation and microwave drying characteristics of beetroot considering energy optimization. Fuel. 2023;346:128345. https://doi.org/10.1016/j.fuel.2023.128345.
48. Tian C, Zhou J, Ren C, Omran M, Zhang F, Tang J. Drying kinetics of microwave-assisted drying of leaching residues from hydrometallurgy of zinc. Materials. 2023;16:5546. https://doi.org/10.3390/ma16165546.
49. Khatun P, Karmakar A, Chakraborty I. Microwave-vacuum drying: Modeling validation of drying and rehydration kinetics, moisture diffusivity and physicochemical properties of dried dragon fruit slices. Food and Humanity. 2024;2:100292. https://doi.org/10.1016/j.foohum.2024.100292.
50. Nigar H, Sturm GSJ, Garcia-Baños B, Peñaranda-Foix FL, Catalá-Civera JM, Mallada R, et al. Numerical analysis of microwave heating cavity: combining electromagnetic energy, heat transfer and fluid dynamics for a NaY zeolite fixed-bed. Appl Therm Eng. 2019;155:226–38. https://doi.org/10.1016/j.applthermaleng.2019.03.117.
51. Aziz NAM, Mohamed H, Ong MY, Yunus R, Law MC, Hamid HA, et al. Numerical simulation of hotspot in polyol ester production using microwave-assisted reaction. Result Eng. 2025;25:104577. https://doi.org/10.1016/j.rineng.2025.104577.
52. Chen J, Pitchai K, Birla S, Jones D, Negahban M, Subbiah J. Modeling heat and mass transport during microwave heating of frozen food rotating on a turntable. Food Bioprod Process. 2016;99:116–27. https://doi.org/10.1016/j.fbp.2016.04.009.
53. Dehghannya J, Habibi-Ghods M. Computer simulation of microwave-assisted drying: coupled influence of microwave power and pulse ratio on product and process characteristics. Curr Res Food Sci. 2025;10:101013. https://doi.org/10.1016/j.crfs.2025.101013.

Publisher's Note Springer Nature remains neutral with regard to jurisdictional claims in published maps and institutional affiliations.